Discontinuous Spectral Element Approach for Solving Transient Radiative Transfer Equation

J.M. Zhao* and L.H. Liu[†]

Harbin Institute of Technology, Harbin 150001, People's Republic of China

Abstract

A discontinuous spectral element method (DSEM) is presented to solve transient radiative heat transfer in multidimensional semitransparent media. The transient term is discretized by Crank-Nicolson scheme, while the spatial discretization is conducted using discontinuous spectral element approach. The salient features of the DSEM are that it possesses high order accuracy, has properties such as local conservation and its solutions are allowed to be discontinuous across interelement boundaries. The inherent discontinuity acceptable property of the DSEM allows efficient and accurate capturing the sharp wave front of transient radiative transfer process. A special treatment for the problem with diffuse irradiation at boundary is presented to mitigate the ray effect encountered in solving the transient radiative transfer equation. The performance of the DSEM is verified by three test cases. The predicted results by the DSEM agree well with reported benchmark solutions in references.

Keywords: Discontinuous Galerkin method; spectral element method; transient radiative transfer.

---

*Ph.D. Candidate, School of Energy Science and Engineering, 92 West Dazhi Street; cxzjm@hit.edu.cn.

[†] Professor, School of Energy Science and Engineering, 92 West Dazhi Street; lhliu@hit.edu.cn, (corresponding author).

Nomenclature

c = Speed of light, m/s

f = Adjustment parameter for temporal discretization

G = Incident radiation, W/m^2

I = Radiative intensity, W/(m^{2}sr)

I_b = Black body radiative intensity, W/(m^{2}sr)

K = The *k*th element

L = Width of slab, side length, m

L_R = Reference scale, m

M = Number of discrete ordinate direction

$\mathbf{n}_{\partial K}$ = Unit outward normal vector of the boundary of element

N_{el} = Total number of elements

N_{sk} = Number of solution nodes on element

N_t = Number of discretized time steps

N_θ = Number of angular discretization for 1-D cases

N_θ^c = Number of equivalent collimated beams

p = Order of polynomial expansion

q_c = Heat flux of collimated irradiation at direction $\mathbf{\Omega}_c$, W/m^2

$\mathbf{q}$ = Heat flux vector

$\mathbf{r}$ = Spatial coordinates vector

s = Lagrange ray coordinates

S = Source term function defined by Eq. (2)

$\tilde{S}$ = Variable defined by Eq. (22)

t = Time, s

t^* = Dimensionless time

T = Temperature, K

β = Extinction coefficient $\beta = (\kappa_a + \kappa_s)$, m^{-1}

$\tilde{\beta}$ = Variable defined by Eq. (21)

δ = Dirac delta function

ε_w = Wall emissivity

ϕ = Nodal basis function

Φ = Scattering phase function

κ_a = Absorption coefficient, m^{-1}

κ_s = Scattering coefficient, m^{-1}

σ = Stefan-Boltzmann constant, $W/(m^2K^4)$

τ_L = Optical thickness, $\tau_L = \beta L$

ω = Single scattering albedo

$\mathbf{\Omega}$ = Unit vector of radiation direction

Ω = Solid angle

Subscripts

B = Direct component

c = Collimated component

d = Diffuse component in collimated irradiation

n = Time step index

S = Diffuse component in diffuse irradiation

i, j = Spatial node index

w = Value at wall

Superscripts

c = Collimated

m = The mth discrete ordinate direction

1. Introduction

In recent years, with the development of some new technologies such as short pulse laser processing of materials [1-3], light-tissue interaction [4-8] and optical imaging [9-12], which often require good understanding of the transient process of radiation transfer, transient radiative transfer in participant media has attracted the interests of many researchers. Because of the existence of transient term, the transient radiative transfer equation (TRTE) has explicitly the property of hyperbolic type equation. As compared to the steady-state radiative transfer equation (RTE), the accurate solution of TRTE is more difficult. Recently, methods for the solution of transient radiative transfer can be mainly put into three classes: 1) probabilistic based methods, such as Monte Carlo method [13-16]; 2) methods based on integral formulation of TRTE, such as integral equation method (IE) [17-19]; and 3) methods based on TRTE in differential form, such as spherical harmonics method [20], discrete ordinates method [21-24], finite volume method [25, 26], finite element method (FEM) [27] and discontinuous finite element method (DFEM) [28]. Monte Carlo method has advantages such as clear physical meaning, good adaptability and reliability, however it requires large amount of computational effort for solution of transient problem. The IE method has good accuracy for the solution of hyperbolic type differential equation, such as it can capture the discontinuous wave front accurately [17], but it is complex to be adapted to the media with anisotropically scattering and relatively difficult to be implemented for the problem with complex geometry. The methods based on differential form of TRTE are efficient and easy to be applied to the problems with complex media and boundary properties, among which the DOM and FVM have received considerable attention. One of the major drawbacks of the already developed DOM and FVM is that they presents relatively large false scattering and the transient wave front can not be captured efficiently and accurately. Similar problem exists in the FEM [27]. The development of method which is stable, with higher order accuracy and less false scattering, and can accurately capture the sharp wave front is still the highlight and needs further contribution. Recently, based on discontinuous Galerkin approach (DG), Liu and Hsu [28] developed and analyzed

transient radiative transfer in graded index media by a DFEM. Their work initially demonstrates that methods based on DG scheme have good adaptability for the solution of transient radiative transfer problem.

The DG approach was first introduced to the community of radiative transfer by Cui and Li [29, 30], they developed a DFEM for solving the steady-state radiative transfer equation. The DG approach has many advantages comparing to the conventional Galerkin method and has been successfully applied to the solution of many physics and engineering problems [31-34]. In DG approach, the inter-element continuity is released and the approximation space composes of discontinuous functions. This property is expected to be ideal for the solution of transient radiative transfer problem, such as to accurately capture the sharp wave front. Introduction and comprehensive review of the DG approach are referred to Cockburn et al. [35, 36]. Spectral element method (SEM) [37] combines the competitive advantages of high order accuracy of spectral method and the flexibility of finite element method. In SEM, the physical domain is broken up into several elements and within each element a spectral representation based on orthogonal polynomials (such as Chebyshev polynomial and Legendre polynomial) is used. However, the traditional SEM are based on global continuous formulation, in which the functions of approximation space are not allowed to be discontinuous across elements, thus lack the salient features of DG based methods. Recently, by combine both the advantages of DG approach and spectral element approximation, Zhao and Liu [38] presented a discontinuous spectral element method (DSEM) for the solution of steady-state radiative transfer problem. The DSEM is stable, of high order accuracy and shows better performance as compared to its counterparts based on continuous scheme, such as Galerkin spectral element method (GSEM) and least squares spectral element method (LSSEM) [39].

By considering valuable properties of the DSEM [38] promising for solution of transient radiative transfer, such as elemental conservative, high order accuracy, and inherent elemental discontinuity acceptable, in this paper, as an extension of the DSEM, a discontinuous spectral element approach for transient radiative transfer is developed. The performances of the DSEM for solving the TRTE are studied and verified. In the following part, first the governing equations for transient radiative transfer are presented. Then the discretization process of governing equation by the DSEM is given. Finally, three test cases are taken to verify the performances of the DSEM for solving the TRTE.

2. Governing Equations

2.1. Transient Radiative Transfer Equation

The TRTE in absorbing, emitting and scattering media can be written as

$$\frac{\partial I(\mathbf{r},\mathbf{\Omega},t)}{c\,\partial t}+\mathbf{\Omega}\bullet\nabla I(\mathbf{r},\mathbf{\Omega},t)+\beta I(\mathbf{r},\mathbf{\Omega},t)=S(\mathbf{r},\mathbf{\Omega},t)\,, \tag{1}$$

where the source function $S(\mathbf{r},\mathbf{\Omega},t)$ is defined as

$$S(\mathbf{r},\mathbf{\Omega},t)=\kappa_a I_b(\mathbf{r},\mathbf{\Omega},t)+\frac{\kappa_s}{4\pi}\int_{4\pi} I(\mathbf{r},\mathbf{\Omega}',t)\,\Phi(\mathbf{\Omega}',\mathbf{\Omega})\,\mathrm{d}\Omega'\,. \tag{2}$$

The initial and the boundary conditions are needed for Eq. (1) to uniquely define a solution. The initial condition is given by

$$I(\mathbf{r},\mathbf{\Omega},0)=I_0(\mathbf{r},\mathbf{\Omega})\,, \tag{3}$$

and the boundary condition prescribed on the inflow boundary ($\mathbf{n}_w\bullet\,\mathbf{\Omega}<0$) is given as

$$I(\mathbf{r}_w,\mathbf{\Omega},t)=\varepsilon_w I_{bw}(\mathbf{r}_w,t)+\frac{1-\varepsilon_w}{\pi}\int_{\mathbf{n}_w\bullet\mathbf{\Omega}'>0} I(\mathbf{r}_w,\mathbf{\Omega}',t)\left|\mathbf{n}_w\bullet\mathbf{\Omega}'\right|\mathrm{d}\Omega'+q_c(\mathbf{r}_w,t)\delta(\mathbf{\Omega}-\mathbf{\Omega}_c)\,, \tag{4}$$

where $q_c(\mathbf{r}_w,t)$ denotes the heat flux of collimated irradiation at direction $\mathbf{\Omega}_c$.

2.2. Treatment of Collimated Irradiation

For collimated irradiation problem, radiative energy concentrates on one direction. As a result, the usually used angular quadrature schemes such as S_N approximation can not be used effectively to do angular integration. The methods based on discrete ordinate equation of Eq. (1) can not work effectively and special treatment to this kind of problem is thus necessary. The commonly taken approach [12, 21] is to decompose the transient radiative intensity to a collimated component and a diffuse component by applying superposition principle to Eq. (1), which is similar to the treatment of steady-state collimated irradiation problem [40]. The radiative intensity is then decomposed as

$$I(\mathbf{r},\mathbf{\Omega},t)=I_c(\mathbf{r},\mathbf{\Omega},t)+I_d(\mathbf{r},\mathbf{\Omega},t)\,, \tag{5}$$

where $I_c(\mathbf{r},\mathbf{\Omega},t)$ denotes the collimated component and $I_d(\mathbf{r},\mathbf{\Omega},t)$ denotes the diffuse component. The collimated component $I_c(\mathbf{r},\mathbf{\Omega},t)$ is governed by

$$\frac{\partial I_c(\mathbf{r},\mathbf{\Omega},t)}{c\,\partial t}+\mathbf{\Omega}\bullet\nabla I_c(\mathbf{r},\mathbf{\Omega},t)+\beta I_c(\mathbf{r},\mathbf{\Omega},t)=\frac{\mathrm{d}I_c(s)}{\mathrm{d}s}+\beta I_c(s)=0\,, \tag{6}$$

which can be solved analytically for its simple form, the solution can be written with Lagrange description as

$$I_c(s)=I_c(0)\exp\left(-\int_0^s\beta(s)\mathrm{d}s\right), \tag{7}$$

where $s=ct$ is the Lagrange coordinates along the ray trajectory and its origin (s=0) is the place where the photon is started. The diffuse component $I_d(\mathbf{r},\mathbf{\Omega},t)$ is governed by

$$\frac{\partial I_d(\mathbf{r},\mathbf{\Omega},t)}{c\,\partial t}+\mathbf{\Omega}\bullet\nabla I_d(\mathbf{r},\mathbf{\Omega},t)+\beta I_d(\mathbf{r},\mathbf{\Omega},t)=S^+(\mathbf{r},\mathbf{\Omega},t) \tag{8a}$$

with boundary condition

$$I_d(\mathbf{r}_w,\mathbf{\Omega},t)=\varepsilon_w I_{bw}(\mathbf{r}_w,t)+\frac{1-\varepsilon_w}{\pi}\int_{\mathbf{n}_w\bullet\mathbf{\Omega}'>0} I(\mathbf{r}_w,\mathbf{\Omega}',t)\left|\mathbf{n}_w\bullet\mathbf{\Omega}'\right|\mathrm{d}\Omega'\,, \tag{8b}$$

where the modified source term $S^+(\mathbf{r},\mathbf{\Omega},t)$ is given by

$$S^+(\mathbf{r},\mathbf{\Omega},t)=\kappa_a I_b(\mathbf{r},\mathbf{\Omega},t)+\frac{\kappa_s}{4\pi}\left[\int_{4\pi} I_d(\mathbf{r},\mathbf{\Omega}',t)\,\Phi(\mathbf{\Omega}',\mathbf{\Omega})\,\mathrm{d}\Omega'+q_c(\mathbf{r},t)\Phi(\mathbf{\Omega}_c,\mathbf{\Omega})\right]. \tag{9}$$

The transient incident radiation distribution function $G(\mathbf{r},t)$ and radiative heat flux distribution function $\mathbf{q}(\mathbf{r},t)$ can be calculated respectively as

$$G(\mathbf{r},t)=\int_{4\pi} I(\mathbf{r},\mathbf{\Omega},t)\;\mathrm{d}\Omega=\int_{4\pi} I_d(\mathbf{r},\mathbf{\Omega},t)\;\mathrm{d}\Omega+q_c(\mathbf{r},t)\,, \tag{10a}$$

$$\mathbf{q}(\mathbf{r},t)=\int_{4\pi} I(\mathbf{r},\mathbf{\Omega},t)\,\mathbf{\Omega}\,\mathrm{d}\Omega=\int_{4\pi} I_d(\mathbf{r},\mathbf{\Omega},t)\,\mathbf{\Omega}\,\mathrm{d}\Omega+q_c(\mathbf{r},t)\mathbf{\Omega}_c\,. \tag{10b}$$

2.3. Special Treatment for Diffuse Irradiation

As being demonstrated in the section 4 of this paper, the direct discretization of Eq. (1) with transient diffuse irradiation will encounter ray effect. The interpretation of this kind of ray effect is illustrated in Fig. 1. A transient diffuse irradiation is suddenly originating from the left wall due to the emission or diffuse reflection of the wall. Consider a point *P* inside the media, at a small instant *t*, only the radiation from a

small strip on the left wall can reach *P*, which makes the transient energy confined to a very small solid angle $\Delta\Omega$ and angular distribution of radiative intensity contain discontinuities as shown in Fig. 1. In this case, the angular distribution of radiative intensity is difficult to be efficiently and accurately integrated by general angular discretization schemes, such as S_N approximation. The inaccuracy in angular integration will then cause ray effect. This is similar to the steady-state case, namely, "diffuse strip loading" case studied by Ramankutty and Crosbie [41], which result in ray effect when solving by the standard discrete ordinates method.

In this section a special treatment is presented to mitigate the ray effect. Based on the idea that the transient directional radiative intensity at any given point inside the media is due to two sources, namely, 1) photons directly originating from the boundary surface and 2) photons being scattered or emitted inside the media, the radiative intensity can be decomposed into the direct and the diffuse components as

$$I(\mathbf{r},\mathbf{\Omega},t) = I_B(\mathbf{r},\mathbf{\Omega},t) + I_S(\mathbf{r},\mathbf{\Omega},t), \tag{11}$$

where $I_B(\mathbf{r},\mathbf{\Omega},t)$ accounts for transient intensity component due to photons directly originating from the boundary surface, and $I_S(\mathbf{r},\mathbf{\Omega},t)$ accounts for transient intensity component due to photons being scattered or emitted inside the media. It should be noted that this kind of approach was initially proposed in the solution of steady-state radiative transfer problems, such as, the modified differential approximation of Olfe [42] and Modest [43], and the modified discrete ordinates methods of Ramankutty and Crosbie [41], which successfully mitigate the ray effects in standard discrete ordinates method.

As defined above, the direct component $I_B(\mathbf{r},\mathbf{\Omega},t)$ is governed by

$$\frac{\partial I_B(\mathbf{r},\mathbf{\Omega},t)}{c\,\partial t} + \mathbf{\Omega}\bullet\nabla I_B(\mathbf{r},\mathbf{\Omega},t) + \beta I_B(\mathbf{r},\mathbf{\Omega},t) = 0, \tag{12a}$$

with boundary condition

$$I_B(\mathbf{r}_w,\mathbf{\Omega},t) = I(\mathbf{r}_w,\mathbf{\Omega},t). \tag{12b}$$

As for the solution of $I_B(\mathbf{r},\mathbf{\Omega},t)$, we consider an approach to equivalently decompose the diffuse irradiation into many collimated beam of different direction, then each collimated irradiation can be solved by Eq. (7) analytically. The diffuse irradiation at the boundary is decomposed into a set of collimated beam of directions $\mathbf{\Omega}_1^c, \mathbf{\Omega}_2^c, ...\mathbf{\Omega}_N^c$, respectively. As a result, the diffuse irradiation is transformed to a set of

collimated irradiation problems. This treatment is similar to the modified discrete ordinates method developed by Ramankutty and Crosbie [41] for solving steady-state radiative transfer problem. Here, the angular discretization and integration of the direct component $I_B(\mathbf{r},\mathbf{\Omega},t)$ takes a way like discrete ordinates approach. The solid angular space is discretized to N directions. The intensity distribution of the *k*th collimated irradiation problem, namely, $I_B(\mathbf{r},\mathbf{\Omega}_k^{\mathrm{c}},t)$ is solved by Eq. (7).

By definition, the diffuse component $I_S(\mathbf{r},\mathbf{\Omega},t)$ is governed by

$$\frac{\partial I_S(\mathbf{r},\mathbf{\Omega},t)}{c\,\partial t}+\mathbf{\Omega}\bullet\nabla I_S(\mathbf{r},\mathbf{\Omega},t)+\beta I_S(\mathbf{r},\mathbf{\Omega},t)=S(\mathbf{r},\mathbf{\Omega},t)\,, \tag{13a}$$

with boundary condition

$$I_S(\mathbf{r}_w,\mathbf{\Omega},t)=0\,. \tag{13b}$$

Here, the source function $S(\mathbf{r},\mathbf{\Omega},t)$ is calculated as

$$S(\mathbf{r},\mathbf{\Omega},t)=\kappa_a I_b(\mathbf{r},\mathbf{\Omega},t)+\frac{\kappa_s}{4\pi}\left[\int_{4\pi} I_d(\mathbf{r},\mathbf{\Omega}',t)\,\Phi(\mathbf{\Omega}',\mathbf{\Omega})\,\mathrm{d}\Omega'+\sum_{k=1}^{N} I_B(\mathbf{r},\mathbf{\Omega}_k^{\mathrm{c}},t)\,w_k^{\mathrm{c}}\,\Phi(\mathbf{\Omega}_k^{\mathrm{c}},\mathbf{\Omega})\right], \tag{14}$$

where w_k^{c} is the quadrature weight of direction $\mathbf{\Omega}_k^{\mathrm{c}}$. Similarly, the transient incident radiation distribution function $G(\mathbf{r},t)$ and radiative heat flux distribution function $\mathbf{q}(\mathbf{r},t)$ are calculated as

$$G(\mathbf{r},t)=\int_{4\pi} I_S(\mathbf{r},\mathbf{\Omega},t)\;\mathrm{d}\Omega+\sum_{k=1}^{N} I_B(\mathbf{r},\mathbf{\Omega}_k^{\mathrm{c}},t)\,w_k^{\mathrm{c}}\,, \tag{15a}$$

$$\mathbf{q}(\mathbf{r},t)=\int_{4\pi} I_S(\mathbf{r},\mathbf{\Omega},t)\,\mathbf{\Omega}\,\mathrm{d}\Omega+\sum_{k=1}^{N} I_B(\mathbf{r},\mathbf{\Omega}_k^{\mathrm{c}},t)\,w_k^{\mathrm{c}}\,\mathbf{\Omega}_k\,. \tag{15b}$$

3. Discontinuous Spectral Element Discretization

3.1. Transient Term

Because transient radiative transfer process often happens in very small time scale, 10^{-8}s or less, the discretization of transient term of Eq. (1) requires much smaller time step. To avoid numerical overflow, Eq. (1) is transformed to its temporal dimensionless form as

$$\frac{\partial I(\mathbf{r},\mathbf{\Omega},t^*)}{\partial t^*}+L_R\mathbf{\Omega}\bullet\nabla I(\mathbf{r},\mathbf{\Omega},t^*)+L_R\beta I(\mathbf{r},\mathbf{\Omega},t^*)=L_R S(\mathbf{r},\mathbf{\Omega},t^*)\,, \tag{16}$$

where t^* is the dimensionless time defined as $t^* = ct / L_R$, and L_R is a reference length. For the problem of collimated irradiation in one dimensional slab, if we choose L_R equal to the width L of the slab, then the value of t^* equals the dimensionless distance of light beam travels in the slab, for example, when t^* =1, light beam will travels to a distance L. In some references, the reference length was also taken as $L_R = \beta^{-1}$ [12, 21, 26]. It can be seen that these two kind of definition is equivalent when βL =1. In order to indicate the wave front of light beam by the value of t^* for good understanding of the transient radiative transfer process, here we take L_R as characteristic length L of the problem.

The temporal dimensionless TRTE Eq. (16) can be written as

$$\frac{\partial I(\mathbf{r},\mathbf{\Omega},t^*)}{\partial t^*} = F[I(\mathbf{r},\mathbf{\Omega},t^*)], \tag{17}$$

where

$$F[I(\mathbf{r},\mathbf{\Omega},t^*)] = -L_R\mathbf{\Omega}\bullet\nabla I(\mathbf{r},\mathbf{\Omega},t^*) - L_R\beta I(\mathbf{r},\mathbf{\Omega},t^*) + L_R S(\mathbf{r},\mathbf{\Omega},t^*). \tag{18}$$

The discretization of transient term can be written in general form as

$$\frac{I_{t^*+\Delta t^*} - I_{t^*}}{\Delta t^*} = f\, F[I_{t^*+\Delta t^*}] + (1-f)F[I_{t^*}], \tag{19}$$

where Δt^* is dimensionless time step and $f \in [0,1]$ is an adjustment parameter. Taking f as $1/2$, $2/3$ and 1, the Crank-Nicolson, Galerkin and fully implicit scheme are obtained respectively. These three schemes are all unconditionally stable, of which the Crank-Nicolson scheme has second order accuracy. Equation (19) can be rewritten as

$$\mathbf{\Omega}\bullet\nabla I_n(\mathbf{r},\mathbf{\Omega}) + \tilde{\beta}_n I_n(\mathbf{r},\mathbf{\Omega}) = \tilde{S}_n(\mathbf{r},\mathbf{\Omega}) \qquad n = 1,\ldots,N_t, \tag{20}$$

where the subscript "*n*" denotes the *n*th time step, N_t is total number of time steps, $\tilde{\beta}_n$ and $\tilde{S}_n(\mathbf{r},\mathbf{\Omega})$ are defined respectively as

$$\tilde{\beta}_n = \frac{1}{L_R \Delta t^* f} + \beta, \tag{21}$$

$$\begin{aligned}\tilde{S}_n(\mathbf{r},\mathbf{\Omega}) = {} & S_n(\mathbf{r},\mathbf{\Omega}) + \left(\frac{1}{f}-1\right) S_{n-1}(\mathbf{r},\mathbf{\Omega}) \\ & -\left(\frac{1}{f}-1\right)\mathbf{\Omega}\bullet\nabla I_{n-1}(\mathbf{r},\mathbf{\Omega}) - \left[\beta\left(\frac{1}{f}-1\right) - \frac{1}{L_R\Delta t^* f}\right] I_{n-1}(\mathbf{r},\mathbf{\Omega})\end{aligned}. \tag{22}$$

It can be seen from Eq. (20) that temporal discretized TRTE can be written in a form like RTE, thus similar approach for solving RTE can be used to solve Eq. (20).

3.2. Discontinuous Spectral Element Discretization

Here, the discontinuous spectral element method [38] is applied to solve the discrete ordinates form of Eq. (20). Chebyshev spectral nodal basis is employed at each element. The radiative intensity field of *n*th time step and direction $\mathbf{\Omega}^m$ can be approximated over element K as

$$I_n^m(\mathbf{r}) \simeq \sum_{i=1}^{N_{sk}} I_{n;i}^m \phi_i(\mathbf{r}), \tag{23}$$

where $I_{n;i}^m$ denotes the radiative intensity on the *i*th node, ϕ_i is the nodal basis of node *i*, and N_{sk} denotes the number of solution nodes on K. For each element K, the discrete ordinates form of Eq. (20) is weighted by ϕ_j and integrated over K using Gauss divergence theorem. This leads to

$$-\int_K I_n^m \mathbf{\Omega}^m \bullet \nabla \phi_j \mathrm{d}V + \int_{\partial K} \widehat{\mathbf{\Omega}^m I_n^m} \bullet \mathbf{n}_{\partial K} \phi_j \mathrm{d}A + \int_K \tilde{\beta}_n I_n^m \phi_j \mathrm{d}V = \int_K \tilde{S}_n^m \phi_j \mathrm{d}V, \tag{24}$$

where superscript "*m*" denotes the discrete ordinates direction, $\mathbf{n}_{\partial K}$ denotes the unit normal vector of the boundary of element K. The numerical flux $\widehat{\mathbf{\Omega}^m I_n^m}$ is modeled by local Lax-Friedrichs scheme as

$$\widehat{\mathbf{\Omega}^m I_n^m} = \mathbf{\Omega}^m \left\{ I_n^m \right\} + \left| \mathbf{\Omega}^m \right| \left[\!\left[I_n^m \right]\!\right] \mathbf{n}_{\partial K}. \tag{25}$$

Here the operator $\{\bullet\}$ and $[\![\bullet]\!]$ denote the mean value and the jump value of arguments across interelement boundary:

$$\left\{ I_n^m \right\} = \frac{1}{2}(I_n^{m,+} + I_n^{m,-}), \qquad \left[\!\left[I_n^m \right]\!\right] = \frac{1}{2}(I_n^{m,+} - I_n^{m,-}), \tag{26}$$

where the superscript operator "+" and "-" denote the values at the boundary inside element K and outside element K, respectively, which are defined respectively as

$$I_n^{m,+} = \lim_{\delta \to 0} I_n^m(\mathbf{r}_{\partial K} - \delta \mathbf{n}_{\partial K}), \qquad I_n^{m,-} = \lim_{\delta \to 0} I_n^m(\mathbf{r}_{\partial K} + \delta \mathbf{n}_{\partial K}). \tag{27}$$

Figure 2 shows the relation of variables defined in the discontinuous spectral element method for good understanding. By substituting Eq. (23) and Eq. (25) into Eq. (24), the final discretization over element K can be simply written as

$$\mathbf{M}_n^m \mathbf{I}_n^m = \mathbf{H}_n^m, \tag{28}$$

where the matrix $\mathbf{M}_n^m$ and $\mathbf{H}_n^m$ are defined respectively as

$$M_{n;ji}^m = -\int_K \phi_i \, \mathbf{\Omega}^m \bullet \nabla \phi_j \mathrm{d}V + \frac{1}{2}\int_{\partial K} \left(\mathbf{\Omega}^m \bullet \mathbf{n}_{\partial K} + \left| \mathbf{\Omega}^m \right| \right) \phi_i \, \phi_j \mathrm{d}A + \int_K \tilde{\beta}_n \, \phi_i \, \phi_j \mathrm{d}V \,, \tag{29a}$$

$$H_{n;j}^m = \int_K \tilde{S}_n^m \, \phi_j \mathrm{d}V - \frac{1}{2}\int_{\partial K} \left(\mathbf{\Omega}^m \bullet \mathbf{n}_{\partial K} - \left| \mathbf{\Omega}^m \right| \right) I_n^{m,-} \phi_j \mathrm{d}A \,. \tag{29b}$$

3.3. Solution procedures

As shown in Eq. (20), the solution of TRTE requires the solution of a RTE like equation at each time step. At each time step, Eq. (20) is solved element by element. On each element, the matrix equations given by Eq. (28) are solved by Gaussian elimination. The implementation of this discontinuous spectral element method can be carried out according to the following routine:

1. Decompose the solution domain with non-overlap elements and generate spectral nodes on each element according to the polynomial order *p*.
2. Initialize radiative intensity field.
3. Loop at each time step, $n = 1, ..., N_t$.
4. If collimated irradiation is considered, then calculate the collimated component $I_c(\mathbf{r}, \mathbf{\Omega}, n\Delta t^*)$ according to Eq. (7).
5. Calculate matrix $\mathbf{M}_n^m$ and $\mathbf{H}_n^m$, solve matrix equation Eq. (28) element by element to solve Eq. (20) on each direction. As for collimated irradiation problem, solve $I_d(\mathbf{r}, \mathbf{\Omega}, n\Delta t^*)$, else for diffuse irradiation, solve $I_S(\mathbf{r}, \mathbf{\Omega}, n\Delta t^*)$. For other case, directly solve the radiative intensity field $I(\mathbf{r}, \mathbf{\Omega}, n\Delta t^*)$.
6. If time loop does not finish go to step 3, else do postprocessing.

The maximum relative error 10^{-4} of incident radiation ($\left\| G_{new} - G_{old} \right\| / \left\| G_{new} \right\|$) is taken as the stop criterion for the solution of Eq. (20) at each time step.

4. Results and Discussion

Three various test cases are selected to check the performances of the DSEM for solving transient

radiative transfer in semitransparent media. The Crank-Nicolson scheme is taken as temporal discretization for all following computation. For the sake of quantitative comparison to the benchmark results, the integration averaged relative error of the DSEM solution is defined as

$$\text{Relative Error } \% = \frac{\int \left| \text{DSEM solution} - \text{Benchmark result} \right| \mathrm{d}x}{\int \left| \text{Benchmark result} \right| \mathrm{d}x} \times 100 . \tag{30}$$

4.1. Case 1: Collimated Irradiation inside Infinite Slab

We consider one dimensional transient radiative transfer in an infinite slab. The media is absorbing and isotropically scattering with scattering albedo of $\omega = 0.5$. The optical thickness based on width L of the slab is $\tau_L = \beta L$ =1. The left boundary ($x/L = 0$) and the right boundary ($x/L = 1$) are black and both the boundaries and the media are kept cold. Initially ($t = 0$), a collimated beam of unit intensity is suddenly irradiated normal to the left boundary and then held constant. The DSEM was applied to solve the incident radiation and radiative heat flux distribution inside the slab. Figure 3 (a) and (b) show the incident radiation and heat flux distribution at different dimensionless time, respectively, and compared to the results obtained by the IE method [17]. In this study, the slab is equally subdivided into 10 elements with 2nd order polynomial approximation used on each element and the angular space is discretized by S_8 approximation. The dimensionless time step is taken as $\Delta t^* = 0.02$. The result obtained by the IE method [17] uses 100 spatial elements with dimensionless time step of $\Delta t^* = 0.01$. By comparison, the results of the DSEM agree with those of the IE method very well. The DSEM shows better performance in capturing the discontinuous wave front.

In order to study the influence of temporal discretization on the DSEM result, Fig. 4 shows the incident radiation distribution of different time obtained by the DSEM with three different time steps, namely, Δt^* =0.01, 0.05 and 0.1, respectively. With the increasing of time step, the accuracy of temporal integration decreases, which results in an increasing of numerical diffusion.

Because of the particularity of discontinuous Galerkin scheme, namely, it only allows discontinuity existing at element boundary, and still uses continuous approximation inside each element. Accuracy of capturing of wavefront is dependent on and limited to the size of element and the time step. To further

study the performance of DSEM when discontinuous wave front does not coincide with element boundary, Fig. 5 (a) and (b) shows the incident radiation distribution and heat flux distribution of different time, respectively. Here, the slab is subdivided into 5 elements with various polynomial order, namely, *p*=4, 8 and 20, and the time step is taken as $\Delta t^* = 0.02$. It can be seen that the wave front is not well captured when t^*=0.3 and 0.9, where the wave front does not coincide with element boundary. However, the discontinuous wave front can be effectively captured with increasing polynomial order in case it does not coincide with element boundary.

4.2. Case 2: Diffuse Irradiation inside One Dimensional Slab

In this case, the configuration and specification of the properties of media and boundaries are same as in the previous case. Initially ($t = 0$), the temperature of the left boundary is suddenly increased to provide a unit radiative power and then hold constant. This case has been studied by several researchers [17, 27, 44] and serves a good test case for verify the performance of numerical method for transient radiative transfer. The DSEM was applied to solve the incident radiation and radiative heat flux distribution inside the slab. Special treatment for diffuse irradiation is used, namely, the diffuse irradiation is equivalently decomposed to many collimated irradiation. In the following analysis, the dimensionless time step of $\Delta t^* = 0.01$ is taken for all the computation in this section.

Figure 6 (a) and (b) show the incident radiation and heat flux distribution at different dimensionless time, respectively, and compared to the results obtained by the IE method [17]. The slab is uniformly subdivided into 10 elements with 4th order polynomial approximation. The diffuse irradiation on the left boundary is decomposed into $N_\theta^c = 200$ directions of collimated beam, these directions are determined by PCA scheme and also for angular integration used in Eq. (15). Angular discretization for solving the diffuse component takes PCA approximation with N_θ=20. As shown in Fig. 6, the DSEM can accurately capture the wave front, the results of the DSEM agree with those of the IE method [17] very well. Figure 7 (a) and (b) shows the incident radiation and heat flux distribution at different dimensionless time, in which 2nd order polynomial approximation for spatial discretization and different angular discretization schemes are used. Even with very rough angular discretization, such as S_4 approximation, the results of the DSEM agree with those of the IE method very well. The influence of number of equivalent beam N_θ^c on the

performance of the DSEM is shown in Fig. 8. When N_θ^c is small, there are non-physical oscillations in the solved incident radiation by the DSEM, but with the increasing of N_θ^c, the oscillations is effectively mitigated.

A comparison of the DSEM solution with and without special treatment for diffuse irradiation is presented in Fig. 9, where the incident radiation distribution at different dimensionless time obtained by the present approach and is compared with the results of the IE method [17]. Here the solutions obtained based on the general governing equation, namely without special treatment for diffuse irradiation, are denoted as GDSEM. Second order approximation is used on each element. It can be seen that the results of the GDSEM exist obvious non-physical oscillations when the angular discretization is rough (N_θ=20), while with angular refinement (N_θ=40) these non-physical oscillations can be mitigated to a large extent, which is attribute to ray effect. However, the results of DSEM are much better than those of GDSEM under the same spatial and angular discretization as compared to the benchmark results obtained using the IE method [17].

To check the efficiency of the DSEM with special treatment, Fig. 10 shows the computational time of both schemes under same spatial discretization, namely, N_{el}=10 and $p=2$, and different angular discretization when dimensionless time are increased to $t^*=1.8$. With the increasing of angular discretization, namely, PCA discretization with N_θ increase from 10 to 40, both the computational time of the DSEM and the GDSEM are linearly increasing. This was because the computational effort of discrete ordinates solution process is proportional to angular discretization. For the DSEM, it requires the solution of two sub problem, namely, the equivalent collimated irradiation problem and the solution of a discrete ordinates equation (13), as a result, the number of beams taken in the special treatment, namely, N_θ^c, will influence the total computational time. This study shows that with the increasing of N_θ^c from 50 to 200, the total computational time increases little. This is attribute to the analytical solution process of the equivalent collimated irradiation is very efficient. Generally, the DSEM is very efficient.

4.3. Case 3: Two Dimensional Irregular Configuration

In this case, the DSEM is applied to transient radiative transfer in a two dimensional irregular enclosure.

The configuration of the enclosure is shown in Fig. 11 (a). The media is absorbing and emitting with absorption coefficient of $\kappa_a = 1\,\mathrm{m}^{-1}$. All the boundaries are black. Initially, the temperature of media and boundary are 0K. When at $t^* = 0$, the media temperature was suddenly increased to T_g and maintained. Three spatial discretization schemes are used to check the performance of the DSEM, namely, (a) 16 regular elements, (b) 16 irregular elements, (c) 64 regular elements, which are shown in Fig. 11. In this study, the time step is taken as $\Delta t^* = 0.01$, 4^{th} order polynomial approximation is used on each element and angular discretization takes S_8 approximation.

Figure 12 shows the dimensionless radiative heat flux along the bottom wall of different time obtained by DSEM with three spatial decomposition schemes shown in Fig. 11 (a)-(c), and compared to the results obtained by FVM [26]. The results of DSEM agree those of FVM [26] very well, even in case of skewed mesh and very less elements. The maximum integral averaged error based on the result of FVM [26] is less than 2%. Generally, the DSEM is effective to solve multidimensional transient radiative transfer problems.

5. Conclusions

A discontinuous spectral element method is presented to solve transient radiative heat transfer in multidimensional semitransparent media. The transient term is discretized by Crank-Nicolson scheme, while the spatial discretization is conducted by the discontinuous spectral element approach. The DSEM is of high order accuracy and has properties such as local conservation and solutions are allowed to be discontinuous across interelement boundaries. The DSEM is demonstrated to be able to efficiently and accurately capture the sharp wave front of transient radiative transfer process. A special treatment for the diffuse irradiation boundary is presented to mitigate the ray effect encountered in general treatment. The predicted results by the DSEM agree well with reported benchmark solutions in references. The DSEM with special treatment for diffuse irradiation effectively mitigated the ray effect and gives very accurate results. Because of high accuracy of spatial discretization, accurate result can be obtained by DSEM even with relatively small number of elements.

Acknowledgements

The support of this work by the National Nature Science Foundation of China (50636010, 50425619) is gratefully acknowledged.

References

[1] Qui, T. G. and Tien, C. L., "Short Pulse Laser Heating in Metals," *Int. J. Heat Mass Transfer*, Vol. 35, No. 3, 1992, pp. 719-726.

[2] Longtin, J. P. and Tien, C. L., "Saturable Absorption During High-Intensity Laser Heating of Liquids," *ASME J. Heat Transfer*, Vol. 118, No. 4, 1996, pp. 924-930.

[3] Kumar, S. and Mitra, K., "Microscale Aspects of Thermal Radiation Transport and Laser Application," *Adv. Heat Transfer*, Vol. 33, 1999, pp. 187-294.

[4] Yamada, Y., "Light-Tissue Interaction and Optical Imaging in Biomedicine," *Annual Review of Heat Transfer* Vol. 6, No. 6, 1995, pp. 1-59.

[5] Popp, A. K., Valentine, M. T., Kaplan, P. D. and Weitz, D. A., "Microscopic Origin of Light Scattering in Tissue," *Appl. Opt.*, Vol. 42, No. 16, 2003, pp. 2871-2880.

[6] Patterson, M. S., Wilson, B. C. and Wyman, D. R., "The Propagation of Optical Radiation in Tissue I. Models of Radiation Transport and Their Application " *Lasers in Medical Science*, Vol. 6, No. 2, 1991, pp. 155-168.

[7] Okada, E., Firbank, M., Schweiger, M., Arridge, S. R., Cope, M. and Delpy, D. T., "Theoretical and Experimental Investigation of near-Infrared Light Propagation in a Model of the Adult Head," *Appl. Opt.*, Vol. 36, No. 1, 1997, pp. 21-31.

[8] Nussbaum, E. L., Baxter, G. D. and Lilge, L., "A Review of Laser Technology and Light-Tissue Interactions as a Background to Therapeutic Applications of Low Intensity Lasers and Other Light Sources," *Physical Therapy Reviews*, Vol. 8, No. 1, 2003, pp. 31-44.

[9] Hebden, J. C., Veenstra, H., Dehghani, H., Hillman, E. M. C., Schweiger, M., Arridge, S. R. and Delpy, D. T., "Three-Dimensional Time-Resolved Optical Tomography of a Conical Breast Phantom," *Appl. Opt.*, Vol. 40, No. 19, 2001, pp. 3278-3287.

[10] Arridge, S. R., "Optical Tomography in Medical Imaging," *Inverse Problem*, Vol. 15, No. 2, 1999, pp. R41-R93.

[11] Fercher, A. F., Drexler, W., Hitzenberger, C. K. and Lasser, T., "Optical Coherence Tomography - Principles and Applications," *Rep. Prog. Phys.*, Vol. 66, No. 2, 2003, pp. 239-303.

[12] Sakami, M., Mitra, K. and Vo-Dinh, T., "Analysis of Short-Pulse Laser Photon Transport through

Tissues for Optical Tomography," *Opt. Lett.*, Vol. 27, No. 5, 2002, pp. 336-338.

[13] Guo, Z., Kumar, S. and San, K., "Multidimensional Monte Carlo Simulation of Short-Pulse Laser Transport in Scattering Media," *J. Thermophys. Heat Transfer*, Vol. 14, No. 4, 2000, pp. 504-511.

[14] Hsu, P.-f., "Effects of Multiple Scattering and Reflective Boundary on the Transient Radiative Transfer Process," *International Journal of Thermal Sciences*, Vol. 40, No. 6, 2001, pp. 539-549.

[15] Gentile, N. A., "Implicit Monte Carlo Diffusion-an Acceleration Method for Monte Carlo Time-Dependent Radiative Transfer Simulations," *J. Comput. Phys.*, Vol. 172, No. 2, 2001, pp. 543-571.

[16] Sakami, M., Mitra, K. and Hsu, P. F., "Analysis of Light-Pulse Transport through Two-Dimensional Scattering and Absorbing Media," *J. Quant. Spectrosc. Radiat. Transf.*, Vol. 73, No. 2-5, 2002, pp. 169-179.

[17] Tan, Z. M. and Hsu, P. F., "An Integral Formulation of Transient Radiative Transfer," *ASME J. Heat Transfer*, Vol. 123, No. 3, 2001, pp. 466-475.

[18] Wu, C. Y., "Propagation of Scattered Radiation in a Participating Planar Medium with Pulse Irradiation," *J. Quant. Spectrosc. Radiat. Transf.*, Vol. 64, No. 5, 2000, pp. 537-548.

[19] Wu, C. Y. and Wu, S. H., "Integral Equation Formulation for Transient Radiative Transfer in an Anisotropically Scattering Medium," *Int. J. Heat Mass Transfer*, Vol. 43, No. 11, 2000, pp. 2009-2020.

[20] Mitra, K. and Kumar, S., "Development and Comparison of Models for Light-Pulse Transport through Scattering-Absorbing Media," *Appl. Opt.*, Vol. 38, No. 1, 1999, pp. 188-196.

[21] Guo, Z. and Kumar, S., "Discrete-Ordinates Solution of Short-Pulsed Laser Transport in Two-Dimensional Turbid Media," *Appl. Opt.*, Vol. 40, No. 19, 2001, pp. 3156-3163.

[22] Guo, Z. and Kumar, S., "Three-Dimensional Discrete Ordinates Method in Transient Radiative Transfer," *J. Thermophys. Heat Transfer*, Vol. 16, No. 3, 2002, pp. 289-296.

[23] Guo, Z. and Kim, K. H., "Ultrafast-Laser-Radiation Transfer in Heterogeneous Tissues with the Discrete-Ordinates Method," *Appl. Opt.*, Vol. 42, No. 16, 2003, pp. 2897-2905.

[24] Mitra, K., Lai, M.-S. and Kumar, S., "Transient Radiation Transport in Participating Media with a Rectangular Enclosure," *J. Thermophys. Heat Transfer*, Vol. 11, No. 3, 1997, pp. 409-414.

[25] Chai, J. C., "One-Dimensional Transient Radiation Heat Transfer Modeling Using a Finite-Volume Method," *Numer. Heat Transfer B*, Vol. 44, No. 2, 2003, pp. 187-208.

[26] Chai, J. C., "Transient Radiative Transfer in Irregular Two-Dimensional Geometries," *J. Quant. Spectrosc. Radiat. Transf.*, Vol. 84, No. 3, 2004, pp. 281-294.

[27] An, W., Ruan, L. M., Tan, H. P. and Qi, H., "Least-Squares Finite Element Analysis for Transient Radiative Transfer in Absorbing and Scattering Media," *J. Heat Transfer*, Vol. 128, No. 5, 2006, pp. 499-503.

[28] Liu, L. H. and Hsu, P.-f., "Analysis of Transient Radiative Transfer in Semitransparent Graded Index Medium," *J. Quant. Spectrosc. Radiat. Transf.*, Vol. 105, No. 3, 2007, pp. 357-376.

[29] Cui, X. and Li, B. Q., "Discontinuous Finite Element Solution of 2-D Radiative Transfer with and without Axisymmetry," *J. Quant. Spectrosc. Radiat. Transf.*, Vol. 96, No. 3-4, 2005, pp. 383-407.

[30] Cui, X. and Li, B. Q., "A Discontinuous Finite-Element Formulation for Internal Radiation Problems," *Numer. Heat Transfer B*, Vol. 46, No. 3, 2004, pp. 223-242.

[31] Bassi, F. and Rebay, S., "High-Order Accurate Discontinuous Finite Element Solution of the 2D Euler Equations," *J. Comput. Phys.*, Vol. 138, No. 2, 1997, pp. 251-285.

[32] Cockburn, B. and Shu, C. W., "The Runge-Kutta Discontinuous Galerkin Method for Conservation Laws V: Multidimensional Systems," *J. Comput. Phys.*, Vol. 141, No. 2, 1998, pp. 199-224.

[33] Baumann, C. E. and Oden, J. T., "A Discontinuous hp Finite Element Method for Convection-Diffusion Problems," *Comp. Meth. Appl. Mech. Eng.*, Vol. 175, No. 3, 1999, pp. 311-341.

[34] Warburton, T. C. and Karniadakis, G. E., "A Discontinuous Galerkin Method for the Viscous MHD Equations," *J. Comput. Phys.*, Vol. 152, No. 2, 1999, pp. 608-641.

[35] Cockburn, B., "Discontinuous Galerkin Methods," *ZAMM*, Vol. 83, No. 11, 2003, pp. 731-754.

[36] Cockburn, B., Karniadakis, G. E. and Shu, C. W. The Development of Discontinuous Galerkin Methods. Berlin: Springer Verlag; 2000: 3-50.

[37] Karniadakis, G. E. and Sherwin, S. J., 1999, *Spectral/hp Element Methods for CFD*, Oxford University Press, New York.

[38] Zhao, J. M. and Liu, L. H., "Discontinuous Spectral Element Method for Solving Radiative Heat Transfer in Multidimensional Semitransparent Media," *J. Quant. Spectrosc. Radiat. Transf.*, Vol. 107, No. 1, 2007, pp. 1-16.

[39] Zhao, J. M. and Liu, L. H., "Least-Squares Spectral Element Method for Radiative Heat Transfer in Semitransparent Media," *Numer. Heat Transfer B*, Vol. 50, No. 5, 2006, pp. 473-489.

[40] Modest, M. F., 1993, *Radiative Heat Transfer*, McGraw-Hill, New York.

[41] Ramankutty, M. A. and Crosbie, A. L., "Modified Discrete Ordinates Solution of Radiative Transfer in Two-Dimensional Rectangular Enclosures," *J. Quant. Spectrosc. Radiat. Transf.*, Vol. 57, No. 11, 1997, pp. 107-140.

[42] Olfe, D. B., "A Modification of the Differential Approximation for Radiative Transfer," *AIAA Journal*, Vol. 5, 1967, pp. 638-643.

[43] Modest, M. F., "Modified Differential Approximation for Radiative Transfer in General Three-Dimensional Media," *J. Thermophys. Heat Transfer*, Vol. 3, No. 3, 1989, pp. 283-288.

[44] Katika, K. M. and Pilon, L., "Modified Method of Characteristics in Transient Radiation Transfer," *J. Quant. Spectrosc. Radiat. Transf.*, Vol. 98, No. 2, 2006, pp. 220-237.

Figure Captions

Figure 1. Schematic interpretation of ray effect in the solution transient radiative transfer problem.

Figure 2. Schematic of variables defined in discontinuous spectral element method.

Figure 3. Solutions obtained by DSEM: **(a)** incident radiation and **(a)** heat flux distribution at different dimensionless time.

Figure 4. The incident radiation distribution of different time obtained with different time steps.

Figure 5. Influence of coincidence of wave front with element boundary and polynomial order on DSEM: **(a)** incident radiation and **(b)** heat flux distribution at different dimensionless time.

Figure 6. Solutions obtained by DSEM: **(a)** incident radiation and **(b)** heat flux distribution at different dimensionless time.

Figure 7. Angular refinement study for DSEM with special treatment for diffuse irradiation: **(a)** the incident radiation and **(b)** heat flux distribution at different dimensionless time.

Figure 8. The influence of number of equivalent beam $N_{\theta'}$ on the performance of the DSEM.

Figure 9. Comparison of the DSEM solution with and without special treatment for diffuse irradiation.

Figure 10. Comparison of computational time of GDSEM and DSEM.

Figure 11. Configuration of irregular quadrilateral enclosure and mesh decomposition and spectral nodes distribution (p=4), **(a)** 16 elements, **(b)** irregular 16 elements, **(c)** 64 elements.

Figure 12. Dimensionless radiative heat flux distributions along the bottom wall of the irregular quadrilateral enclosure at different dimensionless time.

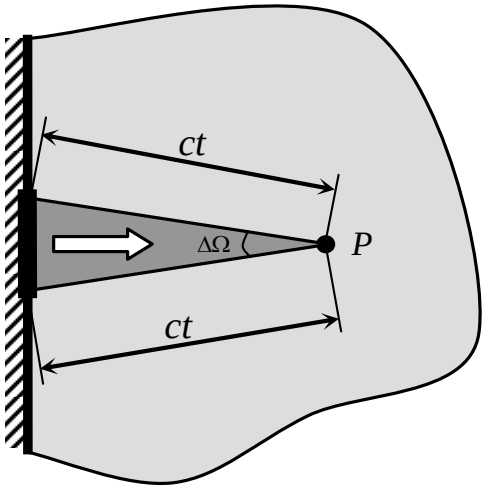

Figure 1

Authors: Zhao and Liu

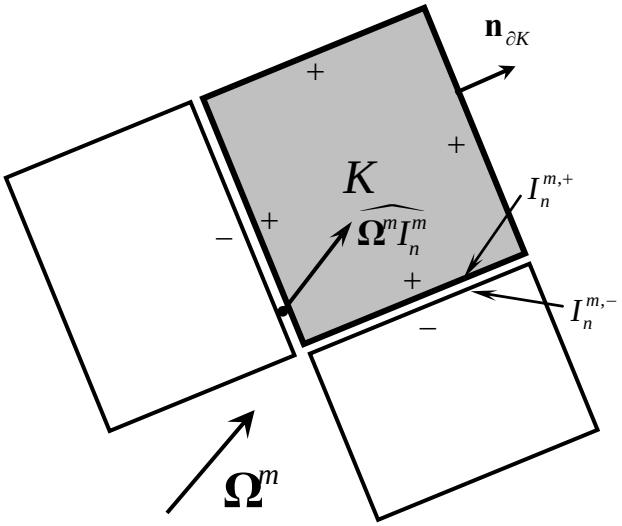

Figure 2

Authors: Zhao and Liu

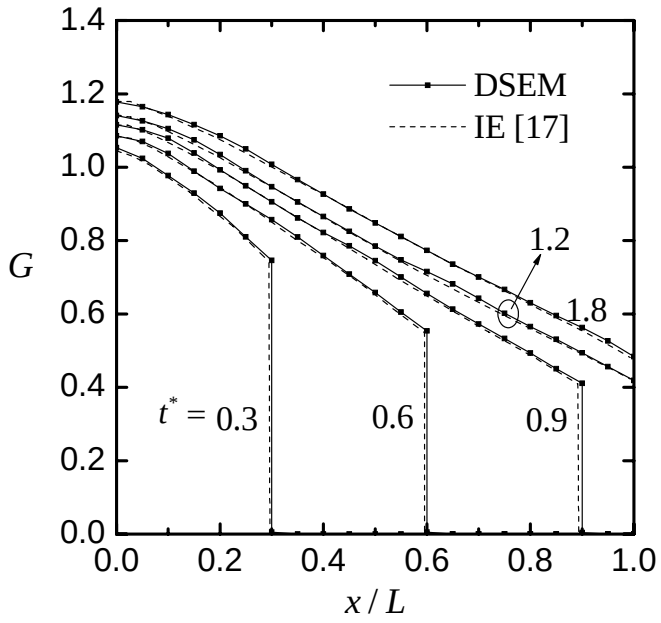

Figure 3 (a)

Authors: Zhao and Liu

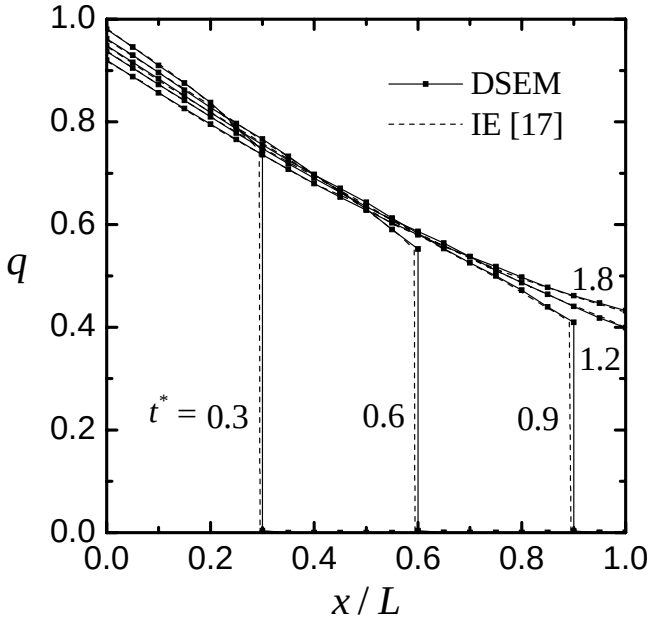

Figure 3 (b)

Authors: Zhao and Liu

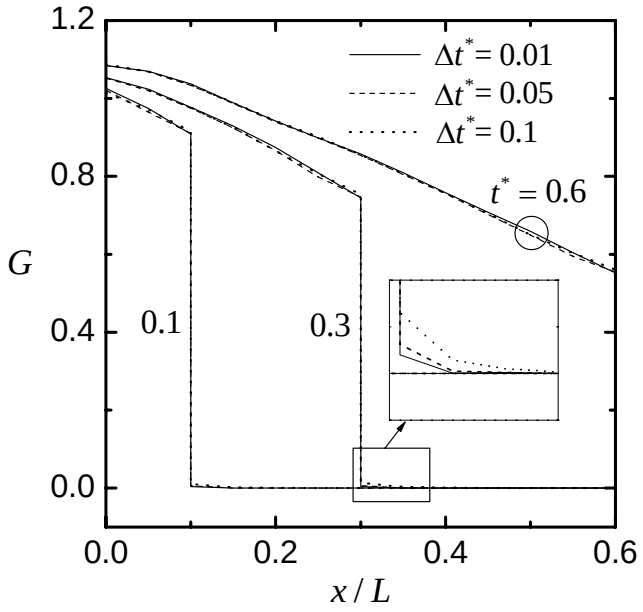

Figure 4

Authors: Zhao and Liu

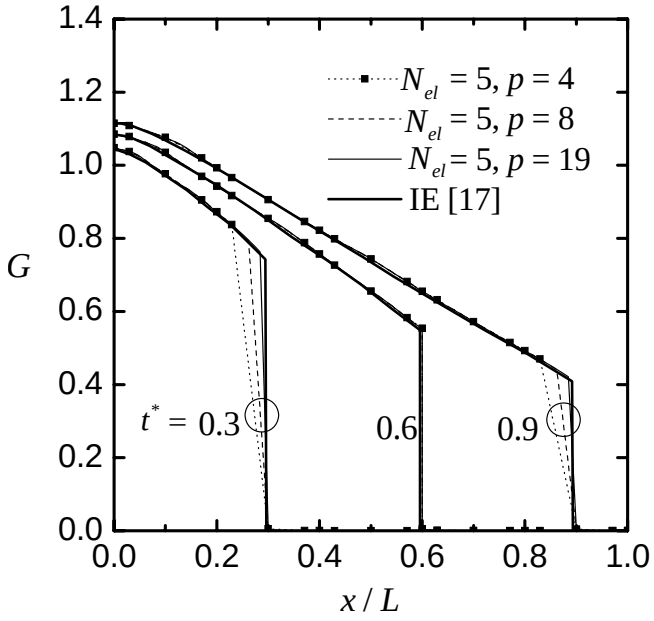

Figure 5 (a)

Authors: Zhao and Liu

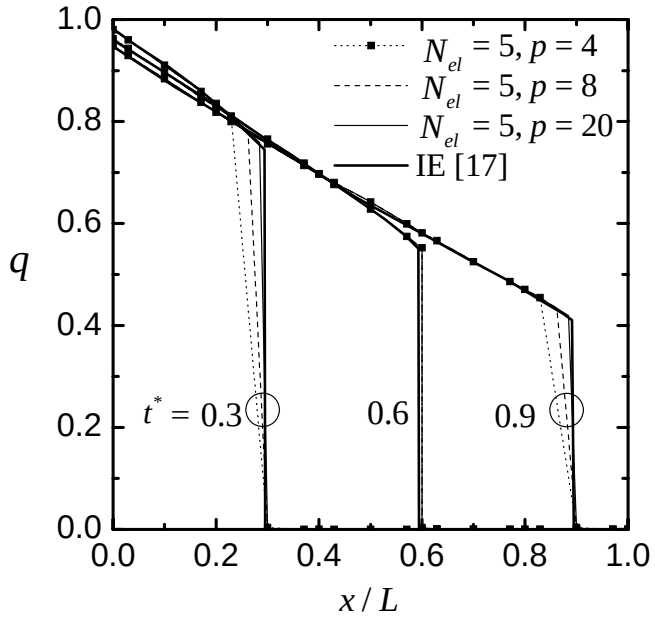

Figure 5 (b)

Authors: Zhao and Liu

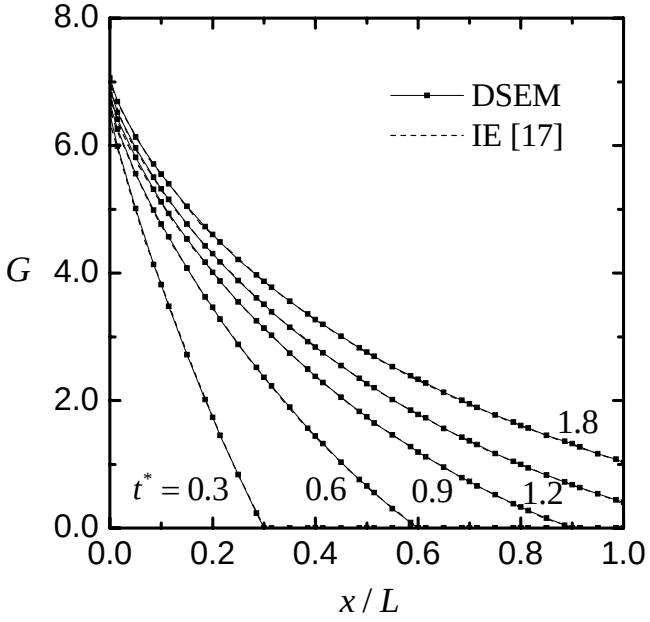

Figure 6 (a)

Authors: Zhao and Liu

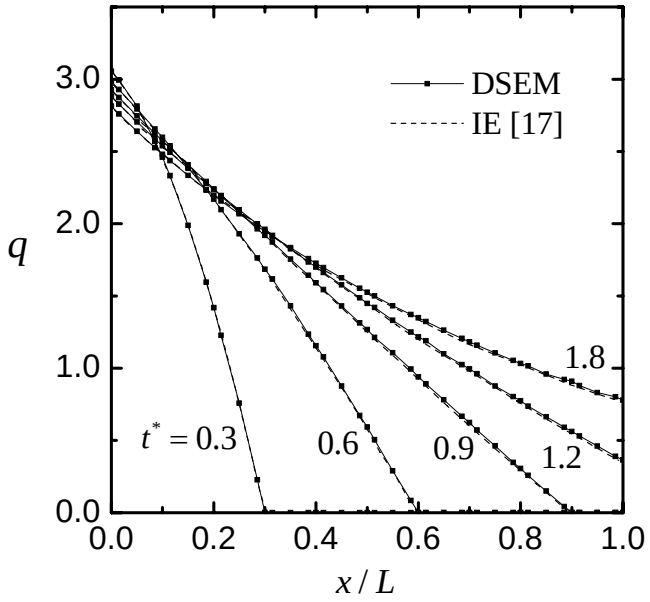

Figure 6 (b)

Authors: Zhao and Liu

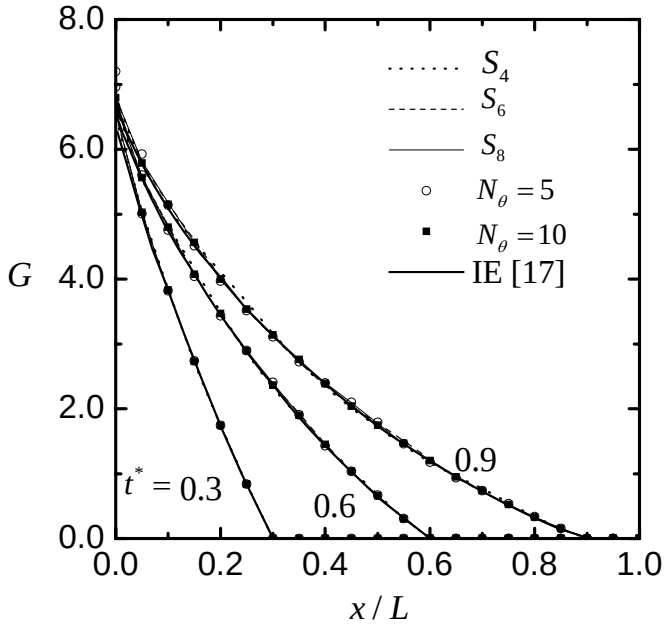

Figure 7 (a)

Authors: Zhao and Liu

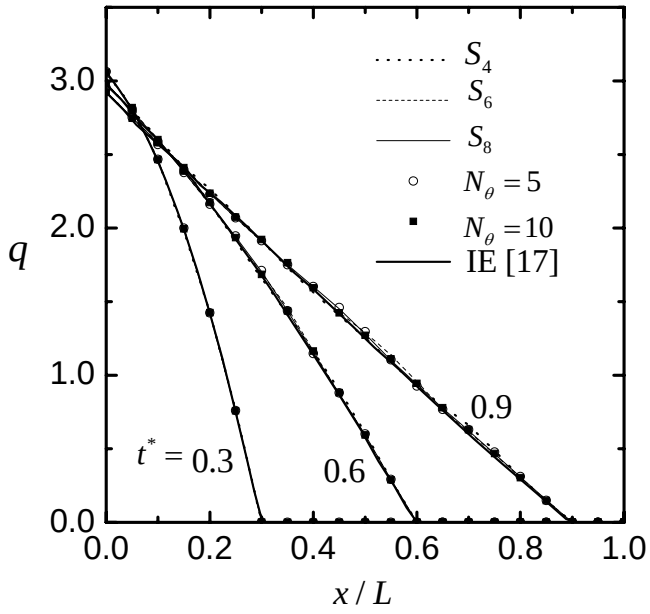

Figure 7 (b)

Authors: Zhao and Liu

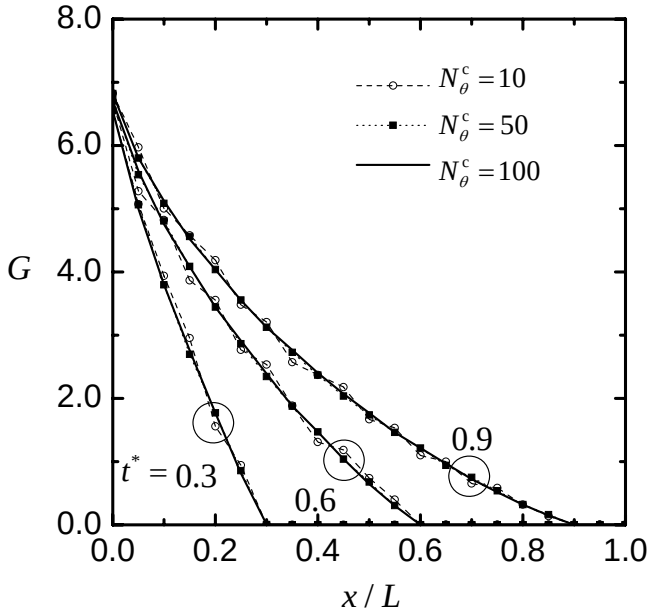

Figure 8

Authors: Zhao and Liu

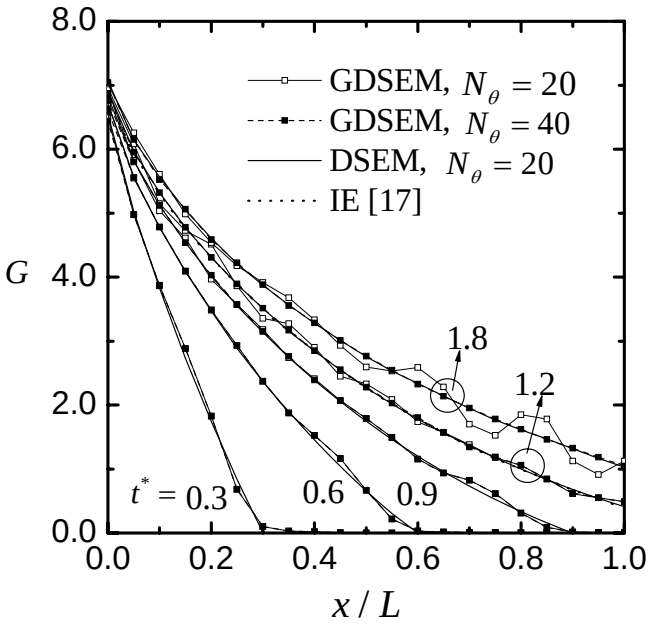

Figure 9

Authors: Zhao and Liu

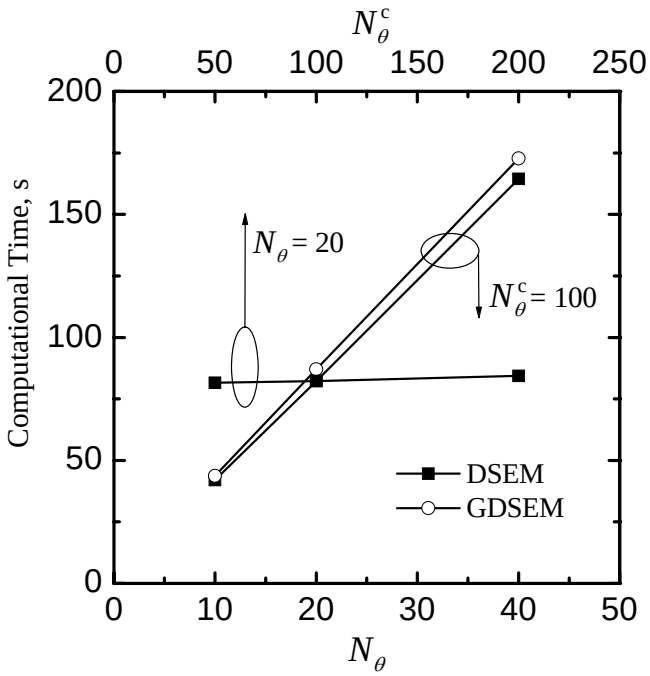

Figure 10

Authors: Zhao and Liu

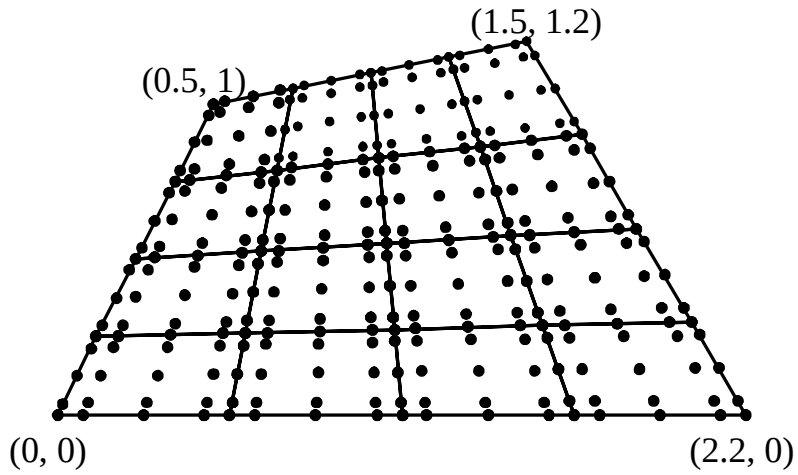

Figure 11 (a)

Authors: Zhao and Liu

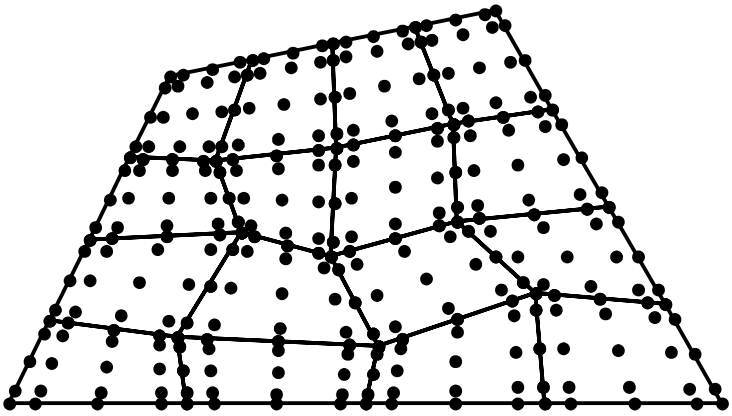

Figure 11 (b)

Authors: Zhao and Liu

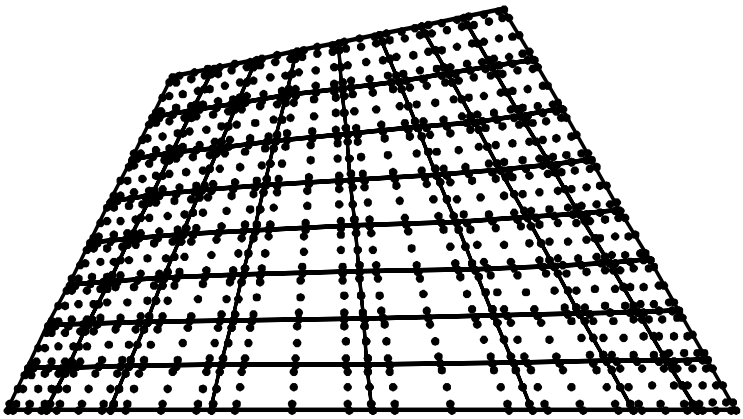

Figure 11 (c)

Authors: Zhao and Liu

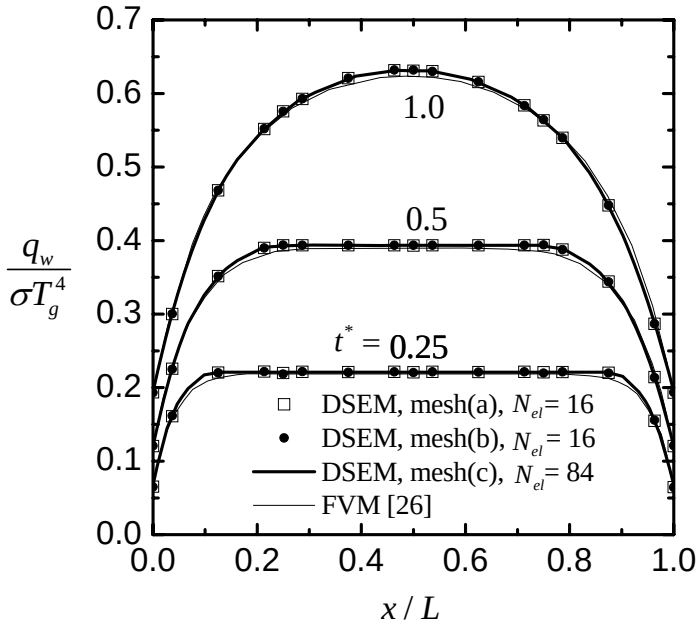

Figure 12

Authors: Zhao and Liu